

Study of kinetics and absorption spectra of OH adducts of hydroxy derivatives of benzaldehyde and acetophenone

S. Geeta^a, S.B. Sharma^a, B.S.M. Rao^{a,*}, H. Mohan^b,
S. Dhanya^b, J.P. Mittal^{b,c}

^a Department of Chemistry, University of Pune, Pune 411 007, India

^b Chemistry Division, Bhabha Atomic Research Centre, Mumbai 400 085, India

^c Jawaharlal Nehru Centre for Advanced Scientific Research, Jakkur Campus, Bangalore 560 064, India

Received 16 October 2000; received in revised form 15 January 2001; accepted 19 January 2001

Abstract

Radiation chemical reactions of $\bullet\text{OH}$, $\text{O}^{\bullet-}$, $\text{N}_3\bullet$ and $\text{SO}_4^{\bullet-}$ with hydroxy derivatives of benzaldehyde and acetophenone were studied. The second-order rate constants for the reaction of $\bullet\text{OH}$ with *o*-, *m*- and *p*-hydroxybenzaldehydes are in the range $(5.2\text{--}12) \times 10^9 \text{ dm}^3 \text{ mol}^{-1} \text{ s}^{-1}$, the order being *para* > *meta* > *ortho*. In $\text{O}^{\bullet-}$ reaction, a reverse trend ($k_{\text{para}} < k_{\text{meta}}$) with much lower rates was noticed. The transient absorption spectra measured in the $\bullet\text{OH}$ reaction with *o*- and *m*-hydroxybenzaldehydes exhibited absorption maxima at 370 and 400 nm, respectively, whereas two peaks centred around 325 and 410 nm were seen in the case of *para* isomer. The absorption at 370 and 325 nm rapidly decayed in *ortho* and *para* isomers, with $k = 5.5 \times 10^5 \text{ s}^{-1}$ in the latter. The spectra measured in the $\bullet\text{OH}$ reaction at 10 μs after the pulse are attributed to the phenoxyl radical formed by dehydration reaction, the rates being dependent on the position of the substituent. The major pathways in the $\text{O}^{\bullet-}$ reaction are electron transfer in the case of the *meta* isomer and addition reaction with the *para* isomer. © 2001 Elsevier Science B.V. All rights reserved.

Keywords: Kinetics; Transient absorption spectra; Benzaldehyde; Acetophenone

1. Introduction

Radiation chemical studies of benzene and its derivatives in aqueous solution (see Refs. [1–4,39,40] for reviews) have provided valuable information on the reactions of both oxidising (e.g. $\bullet\text{OH}$, $\text{SO}_4^{\bullet-}$, $\text{N}_3\bullet$) and reducing radicals (e.g. e_{aq}^- , H and $\text{CO}_2^{\bullet-}$) derived from water radiolysis. The importance of these studies stems from the fact that radiation chemical methods are a clean source for the generation of specific radicals whose yields are precisely known and low solute concentrations of $\leq 10^{-3} \text{ mol dm}^{-3}$ — the normal solubility limit of organic compounds in water — can be easily employed. Furthermore, the pulse radiolysis technique — providing information on the kinetics and spectral nature of the intermediates from optical absorption and conductance detection measurements — combined with product analysis [5,41–44] by the HPLC and GC–MS techniques under steady-state conditions have made these methods particularly unique.

The work of von Sonntag and co-workers [6] on keto–enol tautomerisation of the OH adducts of benzoquinone, oxidation of hydroquinones [7] by $\text{N}_3\bullet$ and OH radical induced oxidation [8,45–47] of phenol and cresols are recent examples of continued interest in radiation chemical oxidation of organic compounds in aqueous solution. Oxidative degradation of benzenes in aqueous solution is another aspect that has been well addressed by the Muelheim group [9,10,48–50] as well as by others [11–13]. Various advanced oxidation processes (e.g. $\text{O}_3\text{--H}_2\text{O}_2$, $\text{H}_2\text{O}_2\text{--UV}$, electron beam) have made use of the high reactivity of the hydroxyl radical in the degradation of water pollutants.

The weakly electrophilic OH radical ($\rho^+ = 0.5$) [14,15] is reactive [1] towards arenes with the k values lying between 10^9 and $10^{10} \text{ dm}^3 \text{ mol}^{-1} \text{ s}^{-1}$ depending on the substituent and it generally reacts by addition [16–19,51–55] to the aromatic ring forming the corresponding hydroxycyclohexadienyl radical. When there is no conjugation with the substituent, the adduct radical exhibits a characteristic absorption in the range 310–320 nm and in conjugated compounds, a red shift in λ_{max} was seen. For instance, λ_{max} values of the OH adducts of benzonitrile and nitrobenzene were reported [1,4,39,40] to be 350 and 410 nm, respectively.

* Corresponding author. Tel.: +91-20-565-6061;
fax: +91-20-565-1728/+91-20-565-3899.
E-mail address: bsmr@chem.unipune.ernet.in (B.S.M. Rao).

Our recent work [20–23,56–62] on radiation induced chemical oxidation of substituted benzenes of the type $C_6H_{5-n}X_nY$ (where $X = H$, halogen or OH and $Y = H$, halogen, $-OCH_3$, $-NH_2$, $-CHO$, $-COCH_3$, $-COC_6H_5$, $-CH_3$, $-CH_2Cl$, $-CHCl_2$ or $-CF_3$) has been undertaken with a view to gain further insight into the reaction mechanism of radiation induced aromatic hydroxylation. Though $\bullet OH$ addition to the benzene ring is the main pathway, our studies [59] on product distribution in chlorotoluenes revealed that H abstraction from the CH_3 group is an additional reaction channel. Similarly, γ radiolysis of benzaldehyde [22,62] has shown the formation of benzoic acid as a major product. Our proposed mechanism involved addition of OH radical to the $-CHO$ group of benzaldehyde followed by disproportionation of the exocyclic OH adduct as its addition to the benzene ring is considerably reduced due to its deactivation by the $-CHO$ group.

In a recent theoretical study of the OH radical reaction with a series of halogenated acetaldehydes, Rayez et al. [24] have shown that the H abstraction from the functional $-CHO$ group is more probable than the addition/elimination reaction. In either case, the formation of an intermediate ketyl radical ($R-\bullet C=O$) is an important step as proposed in autooxidation [25] of aldehydes.

ortho, *meta*, and *para* isomers of hydroxybenzaldehyde and hydroxyacetophenone form an interesting class of compounds to investigate further the $\bullet OH$ reaction mechanism. The deactivation of the ring by the $-CHO$ group is compensated by the activation effect of the $-OH$ group. Since the activation–deactivation effects of the ring by these two groups are different among the three isomers, it is interesting to examine the $\bullet OH$ reaction pattern with these compounds. Recently Solar and Getoff [55] have published their study on reactions of e_{aq}^- with halobenzaldehydes; but to our knowledge, no work on reactions of oxidising radicals with benzaldehyde derivatives has been reported.

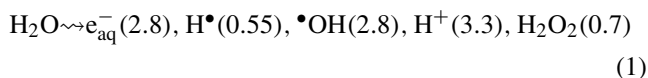
We have, therefore, undertaken a detailed investigation of radiation chemical reactions of $\bullet OH$, $O^{\bullet -}$, and $SO_4^{\bullet -}$ with *o*-, *m*- and *p*-(hydroxybenzaldehydes and hydroxyacetophenones). The semiempirical quantum chemical calculations using the AM1 method were done to determine the charge distribution at different carbon atoms of these compounds.

1.1. Preparation of solutions

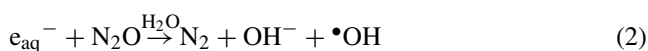
o-, *m*-, and *p*-isomers of hydroxybenzaldehydes and hydroxyacetophenones were obtained from SISCO, CDH and Spectrochem, India. Both *m*- and *p*-(hydroxybenzaldehydes and hydroxyacetophenones) were used as received while their *ortho* isomers were distilled prior to use. The purity of these compounds checked by HPLC was $\geq 98\%$. Fresh solutions, prepared in water purified by the Millipore Milli-Q system, were used. For the spectral measurements, the concentration of the solute was maintained at

$1 \times 10^{-3} \text{ mol dm}^{-3}$ and in kinetics experiments, it was varied from 0.2 to $1 \times 10^{-3} \text{ mol dm}^{-3}$ to evaluate the second-order rate constant.

In radiolysis of water, almost equal amounts of reducing and oxidising radicals are formed (reaction 1) with their *G*-values per 100 eV being given in parentheses.



The reaction of the $\bullet OH$ radical was studied in N_2O saturated solutions containing $1 \times 10^{-3} \text{ mol dm}^{-3}$ solute at pH 6.2 (natural solutions) where e_{aq}^- is quantitatively converted into $\bullet OH$ (reaction 2; $k = 9.1 \times 10^9 \text{ dm}^3 \text{ mol}^{-1} \text{ s}^{-1}$).



Since the pK_a values of *o*-, *m*-, and *p*-hydroxybenzaldehydes are 8.3, 9.0 and 7.6, respectively, they react with the OH radical in their undissociated form.

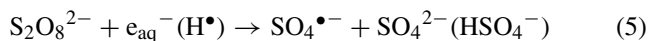
The reaction of $O^{\bullet -}$ was studied in N_2O -saturated basic solutions (pH ~ 13). At this pH, almost all OH radicals are converted into $O^{\bullet -}$ as $pK_a(\bullet OH) = 11.9$ (reaction 3, $k = 1.3 \times 10^{10} \text{ dm}^3 \text{ mol}^{-1} \text{ s}^{-1}$).



N_2O saturated solutions of the substrate containing NaN_3 were radiolysed to produce N_3^\bullet radical (reactions 2 and 4, $k = 1.2 \times 10^{10} \text{ dm}^3 \text{ mol}^{-1} \text{ s}^{-1}$).



$SO_4^{\bullet -}$ radicals were produced by the reaction of e_{aq}^- and H^\bullet with persulphate in N_2 saturated solutions of the solute containing $1.5 \times 10^{-2} \text{ mol dm}^{-3}$ $K_2S_2O_8$ and $2 \times 10^{-4} \text{ mol dm}^{-3}$ *tert*-butyl alcohol (reaction 5, $k(e_{aq}^-) = 1.2 \times 10^{10} \text{ dm}^3 \text{ mol}^{-1} \text{ s}^{-1}$, $k(H^\bullet) = 2.5 \times 10^7 \text{ dm}^3 \text{ mol}^{-1} \text{ s}^{-1}$).



1.2. Irradiation

High-energy electron pulses (7 MeV, 50 ns) from a linear accelerator were used for pulse radiolysis experiments, and the details of the facility are described elsewhere [26]. Dosimetry was carried out with aerated aqueous solutions of $10^{-2} \text{ mol dm}^{-3}$ KSCN by optical measurements taking $G_{\epsilon_{500}} = 21522 \text{ M}^{-1} \text{ cm}^{-1}$ per 100 eV [44] of the transient $(SCN)_2^{\bullet -}$. The dose received per pulse was about 1.2–1.5 krad. The transient absorption spectra were recorded on a digital oscilloscope interfaced to a computer for analysis of kinetics.

2. Results and discussion

2.1. Evaluation of kinetic parameters

2.1.1. Hydroxybenzaldehydes

The rate constants for the reaction of $\bullet\text{OH}$ with isomers of hydroxybenzaldehydes were determined from the growth of the transient band in the solute concentration range $0.2\text{--}1 \times 10^{-3} \text{ mol dm}^{-3}$. The rates of formation of the transients in the case of *ortho* and *meta* isomers were measured at their $\lambda_{\text{max}} = 370$ and 400 nm , respectively. The rate constants were evaluated from the slope of the plot of k_{obs} versus [solute]. The second-order rate constants for the $\bullet\text{OH}$ reaction with *o*- and *m*-hydroxybenzaldehydes were determined to be 5.2×10^9 and $7.7 \times 10^9 \text{ dm}^3 \text{ mol}^{-1} \text{ s}^{-1}$, respectively. The traces depicting the rates of build-up at 370 and 400 nm obtained in the reaction of $\bullet\text{OH}$ with *ortho* and *meta*-hydroxybenzaldehydes, respectively, on $2.5 \mu\text{s}$ scale are shown in insets of Figs. 1 and 2.

In contrast, two absorption maxima at 325 and 410 nm were seen with *p*-hydroxybenzaldehyde. The rate of forma-

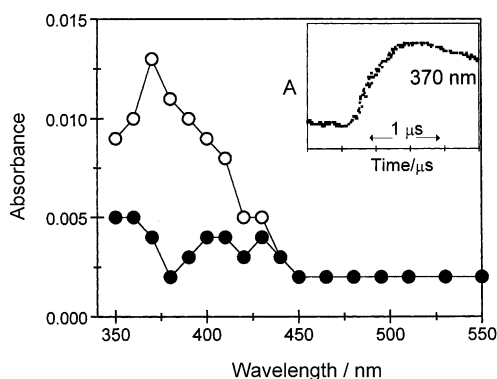


Fig. 1. Time-resolved spectra obtained in the reaction of $\bullet\text{OH}$ with *o*-hydroxybenzaldehyde ($1 \times 10^{-3} \text{ mol dm}^{-3}$), $1.5 \mu\text{s}$ (○) and $15 \mu\text{s}$ (●) after the pulse. Inset: absorption buildup at 370 nm , [*o*-hydroxybenzaldehyde] = $1 \times 10^{-3} \text{ mol dm}^{-3}$; dose/pulse = 1.5 krad .

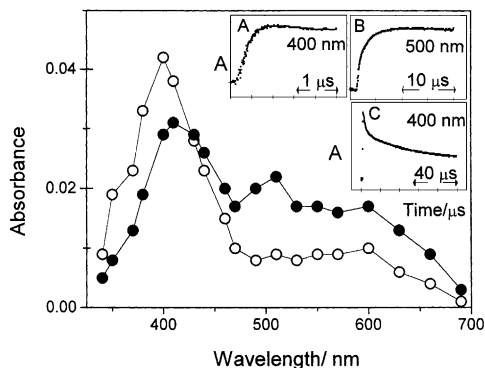


Fig. 2. Time-resolved spectra obtained in the reaction of $\bullet\text{OH}$ with *m*-hydroxybenzaldehyde ($1 \times 10^{-3} \text{ mol dm}^{-3}$), $1.5 \mu\text{s}$ (○) and $15 \mu\text{s}$ (●) after the pulse. Inset: absorption (A) buildup, (B) buildup at 500 nm and (C) decay at 400 nm , [*m*-hydroxybenzaldehyde] = $1 \times 10^{-3} \text{ mol dm}^{-3}$; dose/pulse = 1.5 krad .

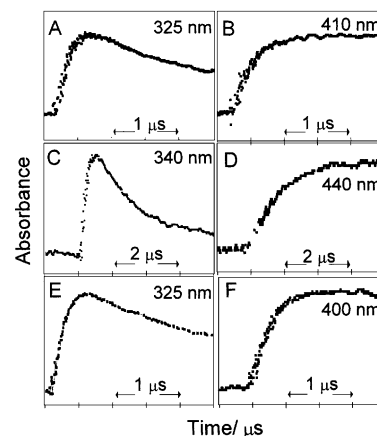


Fig. 3. Absorption traces for the reaction of $\bullet\text{OH}$ with *p*-hydroxybenzaldehyde ($8 \times 10^{-4} \text{ mol dm}^{-3}$) at (A) 325 and (B) 410 nm , $\text{N}_3\bullet$ with *p*-hydroxybenzaldehyde ($1 \times 10^{-3} \text{ mol dm}^{-3}$) at (C) 340 and (D) 440 nm and $\bullet\text{OH}$ with *p*-hydroxyacetophenone ($1 \times 10^{-3} \text{ mol dm}^{-3}$) at (E) 325 and (F) 400 nm .

tion of the transients absorbing at 325 nm was found to be different from that found at 410 nm , the former being much faster than the latter. Furthermore, the growth at 325 nm was followed by a rapid decay. The difference in the rates of formation and decay at 325 and 410 nm indicate that the transients responsible for their absorption are not the same. The appropriate traces at both the wavelengths for [*p*-hydroxybenzaldehyde] = $8 \times 10^{-4} \text{ mol dm}^{-3}$ are shown in Fig. 3A and B. Due to the rapid decay of absorption at 325 nm the second-order rate constant was evaluated by competition kinetics measurements using $1 \times 10^{-4} \text{ mol dm}^{-3}$ KSCN as competitor. The formation of $(\text{SCN})_2\bullet^-$ was monitored at 500 nm in the range [*p*-hydroxybenzaldehyde] = $(0.4\text{--}2.5) \times 10^{-4} \text{ mol dm}^{-3}$ and the second-order rate constant evaluated from this procedure is $1.2 \times 10^{10} \text{ dm}^3 \text{ mol}^{-1} \text{ s}^{-1}$ (inset Fig. 4).

The measured rate constants for all the three hydroxybenzaldehydes ($k = 5.2\text{--}12 \times 10^9 \text{ dm}^3 \text{ mol}^{-1} \text{ s}^{-1}$) are

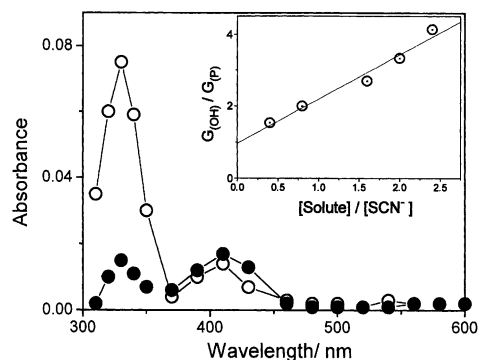


Fig. 4. Time-resolved spectra obtained in the reaction of $\bullet\text{OH}$ with *p*-hydroxybenzaldehyde ($1 \times 10^{-3} \text{ mol dm}^{-3}$), $1.5 \mu\text{s}$ (○) and $10 \mu\text{s}$ (●) after the pulse; dose/pulse = 1.5 krad . Inset: plot for second-order rate constant from competition kinetics.

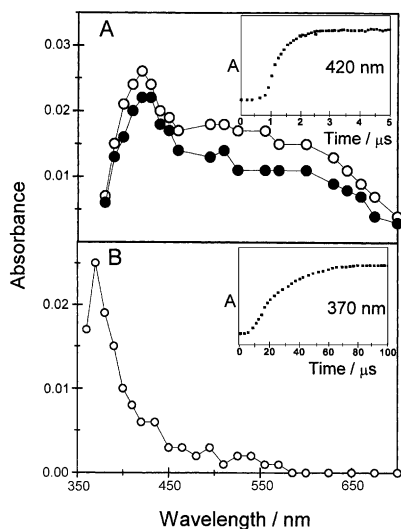


Fig. 5. Transient absorption spectra recorded in the reactions of $\text{O}^{\bullet-}$ with (A) *m*-hydroxybenzaldehyde ($1 \times 10^{-3} \text{ mol dm}^{-3}$), 10 (\circ) and 80 μs (\bullet) after the pulse. Inset: absorption buildup at 420 nm, (B) *p*-hydroxybenzaldehyde ($1 \times 10^{-3} \text{ mol dm}^{-3}$) 90 μs after the pulse. Inset: absorption buildup at 370 nm, dose/pulse = 1.5 krad.

higher than that reported [1,22,23,62] earlier for benzaldehyde ($2.6 \times 10^9 \text{ dm}^3 \text{ mol}^{-1} \text{ s}^{-1}$), but they are comparable to benzophenone ($7.7 \times 10^9 \text{ dm}^3 \text{ mol}^{-1} \text{ s}^{-1}$) and cresols ($\sim 1 \times 10^{10} \text{ dm}^3 \text{ mol}^{-1} \text{ s}^{-1}$). This increase in rate constants in hydroxy derivatives is attributed to the activation of the ring by the electron donating OH group. The observed higher value for the *para* ($1.2 \times 10^{10} \text{ dm}^3 \text{ mol}^{-1} \text{ s}^{-1}$) isomer is due to the significant activation of C_3/C_5 positions by the $-\text{OH}$ and $-\text{CHO}$ groups (vide infra) while in the *ortho* and *meta* isomers a position activated by one substituent is deactivated by the other.

When the reaction was carried out in N_2O -saturated basic solution ($\text{pH} \sim 13$), the reacting species are essentially $\text{O}^{\bullet-}$ and the monoanions of hydroxybenzaldehydes. In basic solution, *o*-hydroxybenzaldehyde gave an intense yellow colour and hence the reaction of O^{\bullet} with this isomer was not studied. The traces depicting the build-up at the respective absorption maxima in the case of *meta* (420 nm) and *para* (370 nm) isomers are given in the insets of Fig. 5A

and B. As can be seen from these traces, the second-order rate constant for the latter ($k = 5.6 \times 10^7 \text{ dm}^3 \text{ mol}^{-1} \text{ s}^{-1}$) is lower by an order of magnitude than that found for the *meta* isomer indicating that the reaction pathways are different. The lower rates for the $\text{O}^{\bullet-}$ reaction than that found for the corresponding $\bullet\text{OH}$ reaction are due to the charge repulsion between the reacting species, $\text{O}^{\bullet-}$ and the monoanion. Such lowering of rates in basic solution was observed [27–29,63] by us earlier in the reactions of $\bullet\text{OH}$, and e_{aq}^- with purine derivatives. The reverse trend in the rates of the $\text{O}^{\bullet-}$ reaction between *meta* and *para* ($k_{\text{meta}} \gg k_{\text{para}}$) isomers is in accord with the nucleophilic nature of $\text{O}^{\bullet-}$ species.

A few experiments were also carried out to study the rates of reaction of N_3^{\bullet} and $\text{SO}_4^{\bullet-}$ with *m*- and *p*-hydroxybenzaldehydes. The observed rate for the N_3^{\bullet} reaction with *p*-hydroxybenzaldehyde ($\lambda_{\text{max}} = 340$ and 440 nm) is similar to that observed at 325 and 410 nm, respectively, in the $\bullet\text{OH}$ reaction as can be seen from the traces depicted in Fig. 3C and D. The transient absorption spectra in the $\text{SO}_4^{\bullet-}$ reaction with both *m*- and *p*-hydroxybenzaldehydes were fully developed within 2 μs indicating that the rates of the reaction are diffusion-controlled ($k \geq 10^9 \text{ dm}^3 \text{ mol}^{-1} \text{ s}^{-1}$).

The accuracy of the rate constants is within $\pm 10\%$ except in the measurements done at only one concentration (values in parentheses) where it is $\pm 20\%$. The rate constant values for benzaldehyde and acetophenone are taken from Refs. [22,62].

2.2. Hydroxyacetophenones

The measured rates for the $\bullet\text{OH}$ reaction with *o*-, *m*- and *p*-hydroxyacetophenones are similar to those found for hydroxybenzaldehydes, e.g. the second-order rate constants evaluated from the absorption traces obtained at their λ_{max} , when N_2O saturated solution containing $1 \times 10^{-3} \text{ mol dm}^{-3}$ *o*-, *m*- or *p*-hydroxyacetophenone were pulse radiolysed, are in the order $(2.5\text{--}3.5) \times 10^9 \text{ dm}^3 \text{ mol}^{-1} \text{ s}^{-1}$. The rate constants observed in this work for the various reacting species along with the absorption maxima of the transients measured in the $\bullet\text{OH}$ reaction are compiled in Table 1.

Table 1
Second-order rate constants ($\times 10^9 \text{ dm}^3 \text{ mol}^{-1} \text{ s}^{-1}$) and λ_{max} (nm) values obtained in this work

Compound	$\bullet\text{OH}$		$\text{O}^{\bullet-}$		$\text{SO}_4^{\bullet-}$		N_3^{\bullet}	
	λ_{max}	k	λ_{max}	k	λ_{max}	k	λ_{max}	k
Benzaldehyde	370	2.6	310	5.5	370	0.7	–	–
<i>o</i> -Hydroxybenzaldehyde	370	5.2	– ^a	–	370	(6.2)	–	–
<i>m</i> -Hydroxybenzaldehyde	400	7.7	420	0.5	410	(4.2)	370	(6.0)
<i>p</i> -Hydroxybenzaldehyde	325, 410	12.1	370	0.056	400	(5.9)	345	(1.9)
Acetophenone	370	3.7	370	0.9	370	1.8	–	–
<i>o</i> -Hydroxyacetophenone	370	2.7	–	–	370	–	–	–
<i>m</i> -Hydroxyacetophenone	400	2.6	–	–	–	–	–	–
<i>p</i> -Hydroxyacetophenone	325, 410	5.1	–	–	–	–	–	–

^a Not measured.

2.3. Transient absorption spectra

2.3.1. Hydroxybenzaldehydes

•OH reaction. The absorption spectra in N₂O-saturated solutions of hydroxybenzaldehydes (1×10^{-3} mol dm⁻³) were monitored in the wavelength region 300–700 nm. The time-resolved spectra obtained in the reaction of •OH with *o*-hydroxybenzaldehyde is shown in Fig. 1. This spectrum exhibited a broad peak centred around 370 nm, the intensity of which almost completely decayed within 10 μs resulting in a featureless spectrum. The spectrum obtained in the •OH reaction with *m*-hydroxybenzaldehyde has a single peak at 400 nm and the absorption intensity at this wavelength is three times higher than that observed in the case of *ortho* isomer. Fig. 2 depicts the time-resolved absorption spectra measured at 1.5 and 15 μs after the pulse. As can be seen from this figure, a decrease in the intensity at 400 nm accompanied by an increase in absorption at 500 nm was noticed at 15 μs after the pulse. The traces for the decay at 400 nm and growth of absorption at 500 nm are shown in the insets of Fig. 2. The rate for the delayed build-up at 500 nm was estimated to be 4.6×10^5 s⁻¹, measured on 20 μs scale. However, the rate of first-order decay at 400 nm is lower with the residual intensity persisting well beyond 100 μs.

The spectral nature for the transients formed in the •OH reaction with *p*-hydroxybenzaldehyde (Fig. 4) is different from that recorded with its *meta* isomer. In addition to the peak around 410 nm, a very intense peak at 325 nm was seen, the ratio of the respective intensities is being 1:4. Furthermore, the peak at 325 nm decayed by more than 75% within 10 μs as can be seen from the spectrum shown in Fig. 4. The average rate for this decay was estimated to be 5.5×10^5 s⁻¹ in the concentration range $4\text{--}8 \times 10^{-4}$ mol dm⁻³. When the spectral measurements were made at pH 4, the decay at 325 nm was complete within 2 μs, ($k = 1.4 \times 10^6$ s⁻¹) indicating that the transformation is acid catalysed.

O^{•-} reaction. The spectra measured in basic (pH~13) N₂O-saturated solution of *m*- and *p*-hydroxybenzaldehydes are shown in Fig. 5. It can be seen that the spectrum in the former case has two peaks at 420 and 500 nm which resembles that recorded in neutral solution after the transformation reaction responsible for the growth at 500 nm (Fig. 5A) is complete. On the other hand, the spectrum obtained in the O^{•-} reaction with *p*-hydroxybenzaldehyde (Fig. 5B) exhibited a single peak at 370 nm, which is different from that measured for the •OH reaction in neutral solution. The time-resolved spectra obtained with both isomers did not reveal any further spectral changes.

N₃[•] and SO₄^{•-} reactions. The spectrum measured in the N₃[•] reaction with *m*-hydroxybenzaldehyde, shown in Fig. 6B, has a peak at 370 nm which decayed within 15 μs. This spectrum is different from that found for the •OH reaction. With the *para* isomer, an intense and sharp peak at 345 nm was seen in the spectrum recorded at 1 μs after the pulse. The absorption of the sharp peak was reduced to 20% within 7 μs (Fig. 6C). The spectrum recorded at 2 μs after

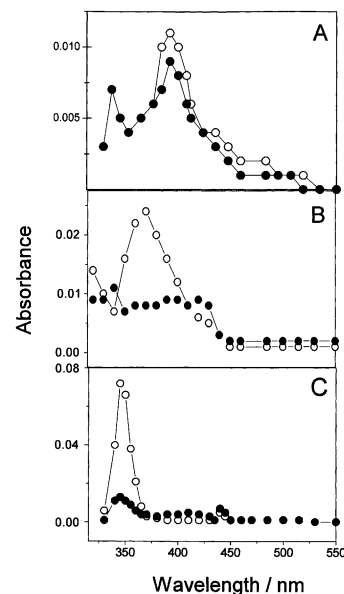


Fig. 6. Transient absorption spectra recorded in the reactions of (A) SO₄^{•-} with *m*-hydroxybenzaldehyde (1×10^{-3} mol dm⁻³), 2 (○) and 40 μs (●), (B) N₃[•] with *m*-hydroxybenzaldehyde (1×10^{-3} mol dm⁻³), 1 (○) and 15 μs (●) and (C) N₃[•] with *p*-hydroxybenzaldehyde (1×10^{-3} mol dm⁻³), 1 (○) and 7 μs (●) after the pulse; dose/pulse = 1.5 krad.

the pulse for transients formed in the SO₄^{•-} reaction with the *meta* isomer has shown two maxima at 330 and 400 nm (Fig. 6A). The spectrum recorded at 40 μs after the pulse has shown the usual bimolecular decay.

2.3.2. Hydroxyacetophenones

The transient absorption spectra in the case of hydroxyacetophenones ($0.5\text{--}1 \times 10^{-3}$ mol dm⁻³) were measured in the wavelength range 300–600 nm. The absorption maxima of transients formed with *o*-, *m*- and *p*-hydroxyacetophenones were found to be similar to those obtained with the corresponding isomers of hydroxybenzaldehydes (Fig. 7). However, the absorption of transients formed in *o*-hydroxyacetophenone (Fig. 7A) persisted even at 40 μs after the pulse unlike in the case of *o*-hydroxybenzaldehyde. The time-resolved spectrum recorded at 500 μs has indicated the usual bimolecular decay. The peak at 400 nm observed in the case of *meta* isomer (Fig. 7B) also decayed with a subsequent build-up at 500 nm similar to that observed with *m*-hydroxybenzaldehyde, the rates of decay and build-up being nearly equal. The rate of decay ($k = 1.9 \times 10^5$ s⁻¹) at 325 nm in the case of *p*-hydroxyacetophenone is lower than that obtained in the case of *p*-hydroxybenzaldehyde ($k = 5.5 \times 10^5$ s⁻¹).

2.4. Semiempirical quantum chemical calculations

The charge distribution at different carbon atoms of the ring and the aldehyde group for isomers of hydroxybenzaldehyde and hydroxyacetophenone was determined using semiempirical quantum chemical calculations. The standard

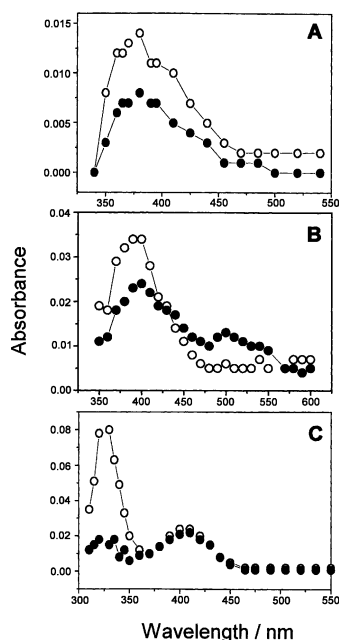


Fig. 7. Time-resolved spectra obtained in the reaction of $\bullet\text{OH}$ with (A) *o*-hydroxyacetophenone ($1 \times 10^{-1} \text{ mol dm}^{-3}$), 3 (\circ) and 40 μs (\bullet), (B) *m*-hydroxyacetophenone ($1 \times 10^{-1} \text{ mol dm}^{-3}$), 2 (\circ) and 40 μs (\bullet) and (C) *p*-hydroxyacetophenone ($1 \times 10^{-1} \text{ mol dm}^{-3}$), 1 (\circ) and 10 μs (\bullet) after the pulse; dose/pulse = 1.5 krad.

AM1 method developed by Dewar et al. [30] was used for optimising the geometry of the molecules with Hartree–Fock approximation. We have also evaluated the charge distribution in benzaldehyde.

The charge densities calculated at different positions are given in Table 2. All the four major rotational conformers of the isomers were considered separately for energy optimisation and the energies were found to be comparable for *meta* and *para* isomers. Therefore, the charge densities of different conformers were averaged for each position. In the *ortho* isomer, however, the conformer with oxygen of $-\text{C}=\text{O}$

and hydrogen of $-\text{OH}$ group adjacent to each other (i.e. hydrogen bonded structure) was found to be much more stable than others. The charge density listed for this isomer corresponds to this structure only.

The analysis revealed that the electron density distribution is in accord with the activation and deactivation effects of the $-\text{OH}$ and $-\text{CHO}$ groups. The probable positions for the $\bullet\text{OH}$ attack are, thus, different for the three isomers. Furthermore, there is no single unique site for the exclusive attack of OH implying the formation of different isomeric OH adducts. A general feature of this analysis is that the electron density at the carbon attached to $-\text{CHO}$ group is significant whereas it is minimum at the exocyclic carbon. The order of the charge distribution at the carbon attached to $-\text{CHO}$, among the three isomers, is *ortho* > *para* > *meta*. Furthermore, the difference in the charge distribution between this and other carbon positions of the ring is the highest in the case of *ortho* isomer, the values being -0.2716 at the former position followed by -0.1822 each at C_3 (*meta* to $-\text{CHO}$ and *ortho* to $-\text{OH}$) and C_5 positions (*meta* to $-\text{CHO}$ and *para* to $-\text{OH}$). In contrast, the charge distribution is almost equally distributed among all ring carbon atoms (-0.1091 to -0.1551) in the case of *m*-hydroxybenzaldehyde, though the carbon bonded to $-\text{OH}$ position ($+0.0657$) is more deactivated than others. In the *para* isomer, C_3/C_5 positions (*meta* to $-\text{CHO}$ and *ortho* to $-\text{OH}$) each has nearly the same value (-0.2026) as that found at the carbon attached to $-\text{CHO}$ (-0.2147).

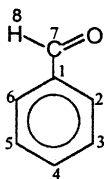
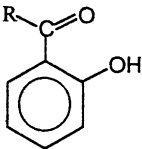
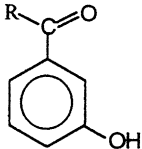
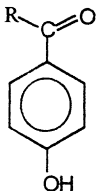
2.5. Reaction mechanism

2.5.1. Hydroxybenzaldehydes

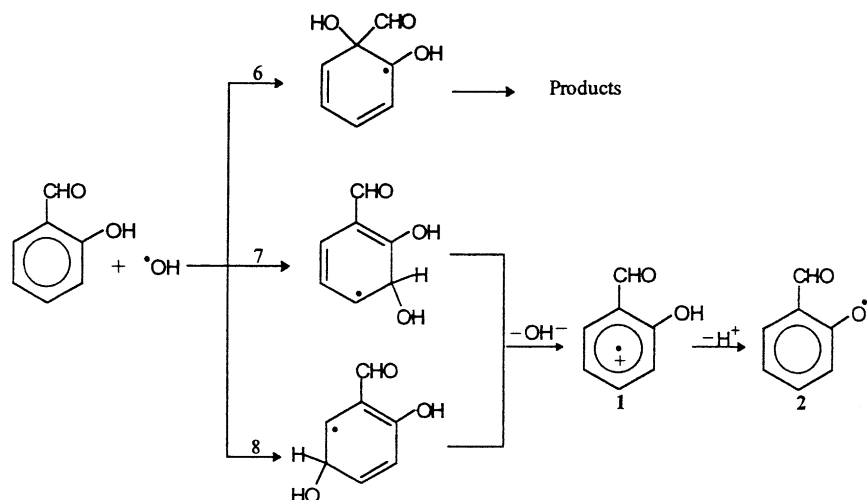
The mechanism for the $\bullet\text{OH}$ reaction of *o*-, *m*- and *p*-hydroxybenzaldehydes can be explained on the basis of the $\bullet\text{OH}$ attack at σ and ipso positions. In the case of *o*-hydroxybenzaldehyde, based on charge distribution (Table 2), the three favourable positions for addition are C_1 , C_3 , and C_5 leading to the formation of the three isomeric OH adducts (reactions 6–8). It is proposed that the two

Table 2

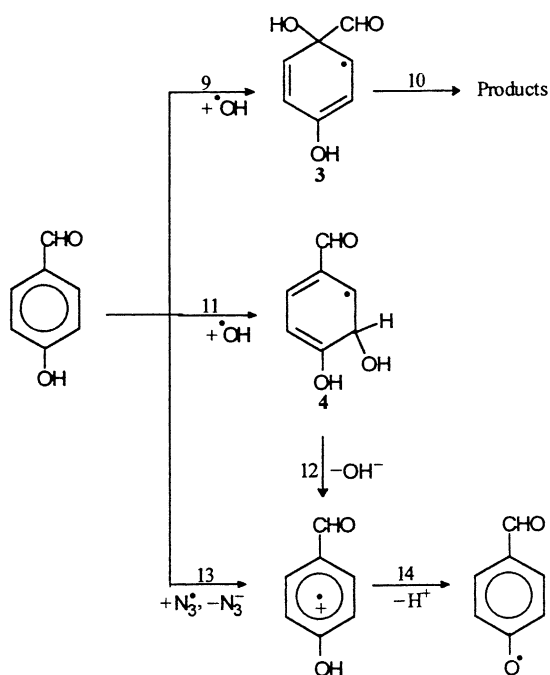
Charge distribution at different carbon atoms in benzaldehyde and hydroxy derivatives of benzaldehyde and acetophenone

							
		R = H	R = CH ₃	R = H	R = CH ₃	R = H	R = CH ₃
1	-0.1773	-0.2716	-0.2490	-0.1410	-0.1201	-0.2147	-0.1938
2	-0.078	+0.1649	+0.1637	-0.1359	-0.1396	-0.0408	-0.0449
3	-0.1452	-0.1822	-0.1825	+0.0657	+0.0654	-0.2026	-0.2020
4	-0.0985	-0.0606	-0.0634	-0.1550	-0.1574	+0.1115	+0.1086
5	-0.1453	-0.1848	-0.1863	-0.1091	-0.1093	-0.2026	-0.2020
6	-0.0780	-0.0509	-0.0556	-0.1143	-0.1181	-0.0408	-0.0449
7	+0.2232	+0.2381	+0.2842	+0.2222	+0.2660	+0.2227	+0.2713
8	-	-	-0.2635	-	-0.2661	-	-0.2659

OH adducts formed from its addition at unsubstituted ring positions lose OH^- followed by deprotonation leading to the formation of $-\text{CHO}$ substituted phenoxyl radical **2** via the intermediate radical cation **1**. The complete decay at 370 nm seen in the absorption spectra (Fig. 1) within $10 \mu\text{s}$ is attributed to this process. The rate of this reaction is estimated to be $3 \times 10^5 \text{ s}^{-1}$.

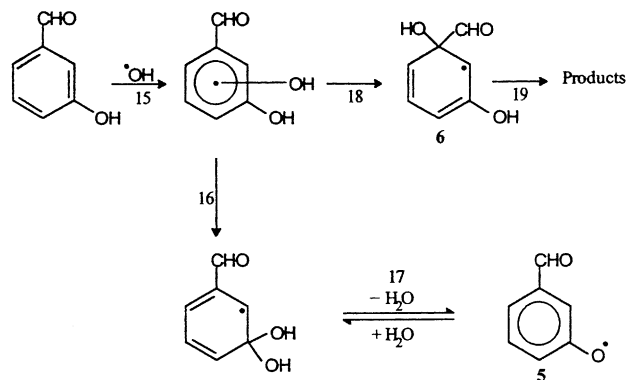


In *p*-hydroxybenzaldehyde, the carbon attached to the $-\text{CHO}$ group and the carbon *meta* to $-\text{CHO}$ and *ortho* to $-\text{OH}$ (C_3 and C_5) are the most favoured sites of attack (Table 2). The scheme depicting the $\cdot\text{OH}$ reaction with *p*-hydroxybenzaldehyde is shown in reactions 9–14, which is similar to the mechanism proposed for the *ortho* isomer. However, the rate of phenoxyl radical formation from the OH adducts of *p*-hydroxybenzaldehyde ($k = 5.5 \times 10^5 \text{ s}^{-1}$) is higher at neutral pH.



This is evident from the time-resolved spectra recorded in *para* and *ortho* isomers where the rate of decay of absorption at 325 nm in the former is higher than that observed in the latter (Figs. 1 and 4). As expected, the OH^- elimination was found to be acid catalysed where the rate was enhanced fivefold at pH 4. Such OH^- elimination was

reported from OH adducts of purines [29] as well as in OH adducts of cresols [8,45–47] and methoxybenzenes [31,64]. The yield of radical cation to that of phenoxyl radical was reported [31,64] to be dependent on the number and position of the methoxyl group. However the radical cation formed from OH^- elimination (reaction 12) from the OH adduct of *o*- or *p*-hydroxybenzaldehydes immediately undergoes deprotonation (reaction 14) as it is unstable due to the electron withdrawing nature of the $-\text{CHO}$ group. This mechanism involving the formation of radical cation is further strengthened from the observed similarity in the nature of absorption spectra measured in $\cdot\text{OH}$ and $\text{N}_3\cdot$ reactions of *p*-hydroxybenzaldehyde (Figs. 4 and 6C).

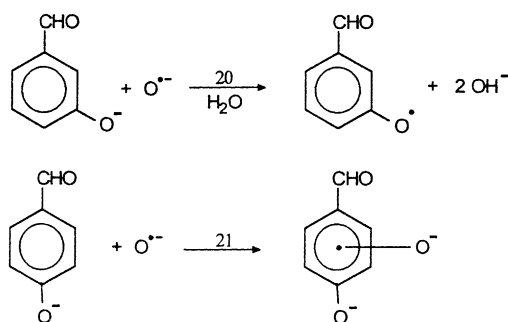


Among the six isomeric OH adducts that are possible in the reaction of $\cdot\text{OH}$ with *m*-hydroxybenzaldehyde (reaction 15), the formation of the adduct from the $\cdot\text{OH}$ attack at the carbon attached to $-\text{OH}$ is more likely due to its activation by both $-\text{CHO}$ and $-\text{OH}$ groups. The other carbon positions

are not activated to the same extent because the position activated by one of the substituents is deactivated by the other. However, this prediction is not supported by the electronic charge distribution value determined for the *meta* position which is positive. Such disagreement was also noticed in our recent study on $\bullet\text{OH}$ reaction with chloroanilines [32]. It, thus, appears that, solvation and other environmental factors [33–35] need to be considered in deciding the reactivity of the intermediates.

The decay of absorption at 400 nm in the transient spectrum with corresponding growth of absorption at 500 nm is attributed to the formation of phenoxyl radical **5** by dehydration of the OH adduct (reaction 17). The rate of water elimination reaction ($k = 4.6 \times 10^5 \text{ s}^{-1}$) from the OH adducts of *m*-hydroxybenzaldehyde is higher by an order of magnitude than that found [31,64] for the OH adducts of methoxybenzene ($k = 4 \times 10^4 \text{ s}^{-1}$) at pH 7. Phenoxyl radicals are known to absorb above 400 nm and no other transformation except the generation of the corresponding phenoxyl radical is likely. The other possibility of the phenoxyl radical formation by elimination of HCHO from the OH adduct **6** is ruled out due to lack of activation at the carbon position attached to the $-\text{CHO}$ group (reaction 18). The assignment of spectrum with absorption maximum at 500 nm to phenoxyl radical thus seems to be reasonable though there is a large red shift as compared to the corresponding radical formed in *p*-hydroxybenzaldehyde and the reasons for this observed difference are not yet clear. It is however, interesting, to note that the absorption maximum of the phenoxyl radicals formed from *meta*-hydroxybenzaldehyde ($\lambda_{\text{max}} = 500 \text{ nm}$) is identical to that reported [36,37] for 4-iodophenoxyl radical, but it shows a red shift compared to other halophenoxyl radicals.

In the $\text{O}^{\bullet-}$ reaction, electron transfer from the phenolate ion to give phenoxyl radical (reaction 20) seems to be favoured in the case of *meta* isomer which is apparent from the



peak observed at 500 nm. However, such an electron transfer with the *para* isomer is not likely due to the stabilisation of the negative charge at the *para* position by $-\text{CHO}$ group and addition to the ring, therefore, seems to predominate. This is supported by the observed low rate of the $\text{O}^{\bullet-}$ reaction with the *para* isomer, since the rate of electron transfer is expected to be higher than the addition reaction [38].

3. Conclusion

$\bullet\text{OH}$ and $\text{N}_3\bullet$ radicals react with hydroxy derivatives of benzaldehyde and acetophenone at diffusion-controlled rates. The electron density distribution in these molecules is in accord with the activation–deactivation effects of the $-\text{OH}$ and $-\text{CHO}$ groups. The subsequent reaction pathways of the adducts radicals following $\bullet\text{OH}$ addition are, thus, different in *ortho*, *meta*, and *para* isomers. The time-resolved spectral changes are interpreted in terms of formation of phenoxyl radical via intermediate radical cation in the case of *ortho* and *para* isomers whereas phenoxyl radical formation by dehydration seems to be the predominant reaction pathway with the *meta* isomer. The OH adducts of hydroxybenzaldehydes are stable against oxidation by $(\text{Fe}(\text{CN})_6)^{3-}$. The major pathways in the $\text{O}^{\bullet-}$ reaction are electron transfer in the case of the *meta* isomer and addition reaction with the *para* isomer. Radiation chemical methods form an excellent tool in the elucidation of oxidation reaction mechanism of disubstituted benzenes especially containing electron donating and electron withdrawing groups.

Acknowledgements

The authors thank Prof. M.S. Wadia for useful discussions and the BRNS, DAE for financial support.

References

- [1] G.V. Buxton, C.L. Greenstock, W.P. Helman, A.B. Ross, J. Phys. Chem. Ref. Data 17 (1988) 513 and the references cited therein.
- [2] P. Neta, R.E. Huie, A.B. Ross, J. Phys. Chem. Ref. Data 17 (1980) 1041.
- [3] S. Steenken, in: E. Minisci (Ed.), Free Radicals in Synthesis and Biology, Nato ASI Series C-260, Kluwer Academic Publishers, Dordrecht, the Netherlands, 1989, p. 213.
- [4] C. von Sonntag, H.-P. Schuchmann, Angew. Chem. Int. Ed. Engl. 30 (1991) 1229.
- [5] R.H. Schuler, L.K. Patterson, E. Janata, J. Phys. Chem. 84 (1980) 2088.
- [6] M.N. Schuchmann, E. Bothe, J. von Sonntag, C. von Sonntag, J. Chem. Soc., Perkin Trans. 2 (1998) 791.
- [7] V.A. Roginsky, L.M. Pisarenko, W. Bors, C. Michel, M. Saran, J. Chem. Soc., Faraday Trans. 94 (1998) 1840.
- [8] M. Roder, L. Wojnarovits, G. Foldiak, S.S. Emmi, G. Beggiato, M. D'Angelantonio, Radiat. Phys. Chem. 54 (1999) 475.
- [9] X.-M. Pan, M.N. Schuchmann, C. von Sonntag, J. Chem. Soc., Perkin Trans. 2 (1993) 289.
- [10] C. von Sonntag, G. Mark, R. Mertens, M.N. Schuchmann, H.-P. Schuchmann, J. Wat. Supply Res. Technol. — Aqua 42 (1993) 201.
- [11] O. Legrini, E. Oliveros, A.M. Braun, Chem. Rev. 93 (1993) 671.
- [12] M.G. Nickelson, W.J. Cooper, K. Lin, C.N. Kurucz, T.D. Waite, Wat. Res. 28 (1994) 1227.
- [13] P.Y. Jiang, Y. Katsumura, R. Nagaishi, M. Domae, K. Ishikawa, Y. Yoshida, J. Chem. Soc., Faraday Trans. 88 (1992) 1653.
- [14] P. Neta, L.M. Dorfman, Adv. Chem. Ser. 81 (1968) 222.
- [15] M. Anbar, D. Meyerstein, P. Neta, J. Phys. Chem. 70 (1966) 2660.
- [16] L.M. Dorfman, I.A. Taub, R.E. Buhler, J. Chem. Phys. 35 (1962) 3051.

- [17] K. Bhatia, R.H. Schuler, *J. Phys. Chem.* 78 (1974) 2335.
- [18] M.K. Eberhardt, *J. Phys. Chem.* 81 (1977) 1051.
- [19] S. Solar, W. Solar, N. Getoff, *Radiat. Phys. Chem.* 28 (1986) 229.
- [20] H. Mohan, M. Mudaliar, C.T. Aravindakumar, B.S.M. Rao, J.P. Mittal, *J. Chem. Soc., Perkin Trans. 2* (1991) 1387.
- [21] G. Merga, C.T. Aravindakumar, H. Mohan, B.S.M. Rao, J.P. Mittal, *J. Chem. Soc., Faraday Trans. 90* (1994) 597.
- [22] S.B. Sharma, M. Mudaliar, B.S.M. Rao, H. Mohan, J.P. Mittal, *J. Phys. Chem. A* 101 (1997) 8402.
- [23] S.C. Choure, M.M.M. Bamatraf, B.S.M. Rao, R. Das, H. Mohan, J.P. Mittal, *J. Phys. Chem. A* 101 (1997) 9837.
- [24] M.T. Rayez, J.C. Rayez, T. Berces, G. Lendvay, *J. Phys. Chem. A* 97 (1993) 5570.
- [25] E.S. Gould, *Organic Reaction Mechanism*, Holt, Rinehart & Winston, New York, 1955, p. 708.
- [26] S.N. Guha, P.N. Moorthy, K. Kishore, D.B. Naik, K.N. Rao, *Proc. Indian Acad. Sci., Chem. Sci.* 99 (1987) 261.
- [27] C.T. Aravindakumar, M. Mudaliar, B.S.M. Rao, H. Mohan, J.P. Mittal, M.N. Schuchmann, B.S.M. Rao, C. von Sonntag, *Int. J. Radiat. Biol.* 66 (1994) 351.
- [28] R.R. Rao, C.T. Aravindakumar, B.S.M. Rao, H. Mohan, J.P. Mittal, *J. Chem. Soc., Faraday Trans. 91* (1995) 615.
- [29] M.S. Vinchurkar, B.S.M. Rao, H. Mohan, J.P. Mittal, K.H. Schmidt, C.D. Jonah, *J. Phys. Chem.* 100 (1996) 9780.
- [30] M.J.S. Dewar, E.G. Zoebisch, E.F. Healy, J.J.P. Stewart, *J. Am. Chem. Soc.* 107 (1985) 3902.
- [31] P. O'Neill, D. Schulte-Frohlinde, S. Steenken, *Faraday Discuss. Chem. Soc.* 63 (1976) 141.
- [32] T.S. Singh, S.P. Gejji, B.S.M. Rao, H. Mohan, J.P. Mittal, unpublished data.
- [33] R.M.W. Wong, K.B. Wilberg, M.J. Frisch, *J. Am. Chem. Soc.* 114 (1992) 523.
- [34] V. Baron, M. Cossi, *J. Phys. Chem. A* 102 (1998) 1995.
- [35] J.B. Foresman, T.A. Keith, K.B. Wilberg, J. Snoonian, M.J. Frisch, *J. Phys. Chem.* 100 (1996) 16098.
- [36] B. Draper, M.A. Fox, E. Pelizzetti, N. Serpone, *J. Phys. Chem.* 93 (1994) 1938.
- [37] J. Lind, X. Shen, T.E. Eriksen, G. Merenyi, *J. Am. Chem. Soc.* 112 (1990) 479.
- [38] P. Neta, R.H. Schuler, *J. Am. Chem. Soc.* 97 (1975) 913.
- [39] C. von Sonntag, H.-P. Schuchmann, in: Z.B. Alfassi (Ed.), *Peroxy Radicals*, Wiley, Chichester, UK, 1997, p. 173.
- [40] H.-P. Schuchmann, C. von Sonntag, in: Z.B. Alfassi (Ed.), *Peroxy Radicals*, Wiley, Chichester, UK, 1997, p. 439.
- [41] E. Janata, R.H. Schuler, *J. Phys. Chem.* 86 (1982) 2078.
- [42] R.H. Schuler, *Radiat. Phys. Chem.* 39 (1992) 105.
- [43] X. Chen, R.H. Schuler, *J. Phys. Chem.* 97 (1993) 421.
- [44] R.H. Schuler, A.L. Hartzell, B. Behar, *J. Phys. Chem.* 85 (1981) 192.
- [45] L. Wojnarovits, A. Kovacs, G. Foldiak, *Radiat. Phys. Chem.* 50 (1997) 377.
- [46] A. Kovacs, K. Gonter, G. Foldiak, I. Gyorgy, L. Wojnarovits, *Models Chem.* 134 (4) (1997) 453.
- [47] M. Roder, G. Foldiak, L. Wojnarovits, *Radiat. Phys. Chem.* 55 (1999) 515.
- [48] X.-M. Pan, M.N. Schuchmann, C. von Sonntag, *J. Chem. Soc., Perkin Trans. 2* (1993) 1021.
- [49] X. Fang, X.-M. Pan, A. Rahmann, H.-P. Schuchmann, C. von Sonntag, *Chem. Eur. J.* 1 (1995) 423.
- [50] C. von Sonntag, *J. Wat. Supply Res. Technol.* — Aqua 45 (1996) 84.
- [51] L.M. Dorfman, R.E. Buhle, I.A. Taub, *J. Chem. Phys.* 36 (1962) 549.
- [52] M.K. Eberhardt, *J. Phys. Chem.* 79 (1975) 1767.
- [53] K. Sehested, H. Corfitzen, H.C. Christensen, E.J. Hart, *J. Phys. Chem.* 79 (1975) 310.
- [54] M.K. Eberhardt, M.I. Martinez, *J. Phys. Chem.* 79 (1975) 1917.
- [55] S. Solar, N. Getoff, *J. Phys. Chem.* 99 (1995) 9425.
- [56] H. Mohan, M. Mudaliar, B.S.M. Rao, J.P. Mittal, *Radiat. Phys. Chem.* 40 (1992) 513.
- [57] M. Mudaliar, Ph.D. Thesis, University of Pune, India, 1993.
- [58] G. Merga, B.S.M. Rao, H. Mohan, J.P. Mittal, *J. Phys. Chem.* 98 (1994) 9158.
- [59] G. Merga, H.-P. Schuchmann, B.S.M. Rao, C. von Sonntag, *J. Chem. Soc., Perkin Trans. 2* (1996) 551.
- [60] G. Merga, H.-P. Schuchmann, B.S.M. Rao, C. von Sonntag, *J. Chem. Soc., Perkin Trans. 2* (1996) 1097.
- [61] G. Merga, Ph.D. Thesis, University of Pune, India, 1995.
- [62] S.B. Sharma, Ph.D. Thesis, University of Pune, India, 1998.
- [63] M.S. Vinchurkar, B.S.M. Rao, H. Mohan, J.P. Mittal, *J. Chem. Soc., Perkin Trans. 2* (1999) 609.
- [64] S. Steenken, *J. Chem. Soc., Faraday Trans.* 87 (1987) 113.